nature communications

Article

https://doi.org/10.1038/s41467-026-74914-z

Ecological multifunctionality of watersheds increases with tree species richness

Received: 12 December 2024

Accepted: 18 June 2026

Published online: 27 June 2026

Check for updates

Jiehao Zhang[1], Peter B. Reich[2,3,4], Conghe Song[5], Yulong Zhang[6,7], Han Y. H. Chen[8], Gert-Jan Nabuurs[9], Xia Wang[1,10], Tiehu He[1,11], Jiri Dolezal[12], Michael Scherer-Lorenzen[13], Alain Paquette[14], Helder Viana[15,16], Giorgio Alberti[17], Elena Parfenova[18], Nadezhda Tchebakova[18], Jingjing Liang[19], Thomas W. Crowther[20], Sergio de-Miguel[21,22], Sebastian Pfautsch[23], Peter Schall[24], Bogdan Jaroszewicz[25], Pablo L. Peri[26], Nicolas Picard[27], Quanfa Zhang[1,10] ✉ & Kerong Zhang[1,28] ✉

Watersheds are natural units and meta-ecosystems of the earth's land surface providing multiple ecological functions. However, little is known about the biodiversity-ecological multifunctionality relationships of watersheds, particularly regarding how these relationships scale to large and complex landscapes. Here, we explore the impact of forest tree species richness on the ecological multifunctionality of watersheds in terms of carbon sequestration, carbon storage, water supply, water regulation, and soil conservation, by utilizing integrated ground-sourced forest inventory datasets comprising 846 forest watersheds from the Global Forest Biodiversity Initiative, the Global Streamflow Indices and Metadata Archive, and remote sensing data products. We find a consistently positive relationship between forest tree species richness and watershed ecological multifunctionality by accounting for factors such as forest structural characteristics and environmental conditions. Furthermore, we find that this biodiversity-multifunctionality link is dependent on spatial scale and climatic context, becoming stronger in larger watersheds but diminishing in arid climatic conditions. These insights enhance our understanding of ecosystem multifunctionality and underscore the importance of considering watershed-scale ecological processes and biodiversity in ecosystem management and conservation strategies.

Concerns over the consequences of accelerating biodiversity loss and global environmental change for human well-being have led to the biodiversity-ecosystem functioning (BEF) becoming a prominent research theme and social hot spot[1,2]. Numerous small-scale manipulated experiments and local surveys have explored the relationships between biodiversity and individual ecological functions (e.g., productivity, biomass storage, and carbon sequestration)[3–5], and in recent years, the ecosystem multifunctionality—the ability of ecosystems to provide multiple functions and services simultaneously[6], attracts increasing attention from researchers and policymakers. When extending BEF to multifunctionality, some patterns identified in single-function BEF research may no longer be applicable[7]. For instance, although positive BEF relationships are commonly observed in single-function BEF research[8,9], a systematic review study found that, in naturally assembled communities, the neutral relationships between biodiversity and ecological multifunctionality were even more

A full list of affiliations appears at the end of the paper. ✉e-mail: qzhang@wbgcas.cn; kerongzhang@wbgcas.cn

prevalent[10]. Another significant challenge is determining whether the findings about BEF obtained from small-scale manipulated experiments and local surveys still hold true at larger spatial scales[10–13], where ecosystems form meta-ecosystems with greater heterogeneity and the ecological functions and services more comprehensively reflect the complexity and reality of Earth's land surface[14,15]. These knowledge gaps not only hinder a broader comprehension of BEF and natural systems but also impede the application of biodiversity theory to policy and management at larger spatial scales.

Watersheds are the natural units and meta-ecosystems of the earth's land surface, providing multiple ecological functions, e.g., carbon sequestration and storage, water supply, water regulation, and soil conservation. The watershed-scale biodiversity-functioning relationship is particularly valuable for informing management and conservation strategies, as watersheds define natural boundaries for the flow of water and nutrients[16], making them critical units for ecological planning and policy implementation. In a relatively uniform ecosystem, which is often selected for ecological studies and manipulated experiments, ecological functions may be simply additive[17] and may be influenced by localized factors, such as soil type, microclimate, and species interactions[18–20]. Watersheds are meta-ecosystems and encompass a broader range of ecological processes and interactions due to their larger spatial extent and diverse environmental gradients[16,21,22]. Hydrological processes at the watershed scale determine the movement of water[23], acting as carriers of energy and material spatial flows that connect a set of ecosystems within[24]. Some watershed functions driven by hydrological processes, such as water supply and regulation, emerge primarily at the watershed scale, while do not fully manifest at the plot scale. Multiple ecosystems within a watershed cause great heterogeneity in vegetation, land-use, soil property, and topography[21]. These heterogeneities can create mosaic habitats and diverse microenvironments, leading to greater heterogeneity in ecological functions[25], that are not evident at smaller scales[26]. In addition, the connected ecosystems within watersheds provide the cumulative effects on multiple ecological functions, including element cycling, hydrological regulation, and soil conservation[27,28]. Therefore, the biodiversity-ecological multifunctionality relationships of watersheds are expected to be highly complex and elusive. Currently, the effects of plant biodiversity on watershed ecological multifunctionality remain unknown. Understanding biodiversity-ecological multifunctionality relationships at the watershed scale can provide deeper insights into ecological processes and contribute to more robust theories under real Earth's surface environmental conditions[12].

Here, we explore the impacts of forest tree species richness on the ecological multifunctionality of watersheds. We utilize integrated datasets from the Global Forest Biodiversity Initiative[9], the Global Streamflow Indices and Metadata Archive[29,30], and up-to-date remote sensing data products. Through rigorous data screening ("Materials and Methods"), we obtain 846 forest watershed samples (Fig. 1) containing 55,337 spatially referenced forest plots with an average size of approximately 900 m^2, which are primarily concentrated in the eastern United States, with a smaller number of watersheds in Europe and Japan, mostly distributed between 30°N and 45°N. We consider five categories of ecological functions (i.e., carbon sequestration, carbon storage, water supply, water regulation, and soil conservation) based on 11 independent measurements (i.e., net carbon accumulation rate in tree stem, carbon assimilation rate, biomass storage, soil organic carbon, minimum water supply capacity, water supply stability, runoff coefficient, evapotranspiration, flood control, surface soil water content, and soil stability) (Fig. S3 and Table S1). We quantify multifunctionality across these watersheds using three methods, i.e., averaging, principal component analysis (PCA), and multi-threshold methods. We examine the relationship between the quadrat-based tree species richness index and multifunctionality ecological indices of watersheds, as well as the individual ecological functions, considering other potential drivers of watershed multifunctionality, such as forest structural characteristics and environmental conditions (i.e., climate, soil, and topography). Moreover, we explore the influence of watershed area and climate context on the relationship between forest tree species richness index and watershed multifunctionality. Our findings highlight the robust positive correlation between tree species richness and watershed ecological multifunctionality, while multifunctionality is significantly influenced by canopy cover fraction and various environmental factors. Furthermore, we find that this biodiversity-multifunctionality link is dependent on spatial scale and climatic context, becoming stronger in larger watersheds but diminishing in arid climatic conditions.

Results and discussion

Tree species richness-watershed ecological multifunctionality relationships

We employed partial correlation analysis to evaluate the independent effect of tree species richness on ecological multifunctionality while accounting for confounding environmental and structural factors. Tree species richness exhibited a consistent and significant positive correlation with watershed ecological multifunctionality across all calculation methods employed (Fig. 2a–f). Specifically, relationships controlling for forest structure, climatic, soil, and topographic covariates showed significant positive associations with multifunctionality (Fig. 2a–f). For instance, tree species richness was positively associated with the mean-based (effect size $R_{resid} = 0.19$, 95% CI = 0.12–0.25, $t(844) = 5.63$, $p < 0.001$) and PCA-based multifunctionality indices (effect size $R_{resid} = 0.20$, 95% CI = 0.14–0.26, $t(844) = 5.94$, $p < 0.001$). The relationship remained particularly robust for multifunctionality indices using 20% (effect size $R_{resid} = 0.22$, 95% CI = 0.16–0.28, $t(844) = 6.59$, $p < 0.001$) to 60% (effect size $R_{resid} = 0.27$, 95% CI = 0.20–0.33, $t(844) = 8.07$, $p < 0.001$) thresholds of the multi-threshold method compared to the other multifunctionality indices (Figs. 2c–f and S4). Correlation analysis based on successive thresholds showed that multi-threshold-based multifunctionality indices with thresholds between 40 and 60% were the most sensitive to changes in the tree species richness index, whereas the influence of species richness diminished substantially at higher thresholds (e.g., >70%) (Fig. S4). Among forest structural parameters, the canopy cover fraction and tree density showed the strongest correlation with ecological multifunctionality indices (Figs. 2g and S5). In comparison, canopy height had weaker relationships with watershed ecological multifunctionality (Figs. 2g and S5).

To quantify the relative contributions of biotic and abiotic drivers under a multivariate framework, we utilized ordinary least squares (OLS) regression models (Fig. 3a, b, and Tables S4, S5). To eliminate inherent collinearity between biodiversity and forest structure, we used the residuals of tree species richness (regressed against all other environmental and structural predictors) as the primary biodiversity metric. The relative importance of tree species richness ranged from 5.3 to 13.7% across multifunctionality indices (Fig. 3 and Tables S4, S5). Tree species richness had a relative importance exceeding 10% across thresholds ranging from 20 to 70% in the multi-threshold analysis (Fig. 3d). To further address potential multicollinearity among regression predictors and provide more robust coefficient estimates, we performed Ridge regression to compare the standardized effects of tree species richness index and specific structural parameters (Fig. 3c and Tables S6, S7). The Ridge regression models further confirmed that tree species richness index and canopy cover were the most prominent biotic drivers of multifunctionality for both the mean-based and PCA-based multifunctionality indices (Fig. 3c).

Our findings provide empirical evidence that the positive link between biodiversity and ecological multifunctionality remains robust at the watershed scale. Specifically, we observed a robust and

https://doi.org/10.1038/s41467-026-74914-z

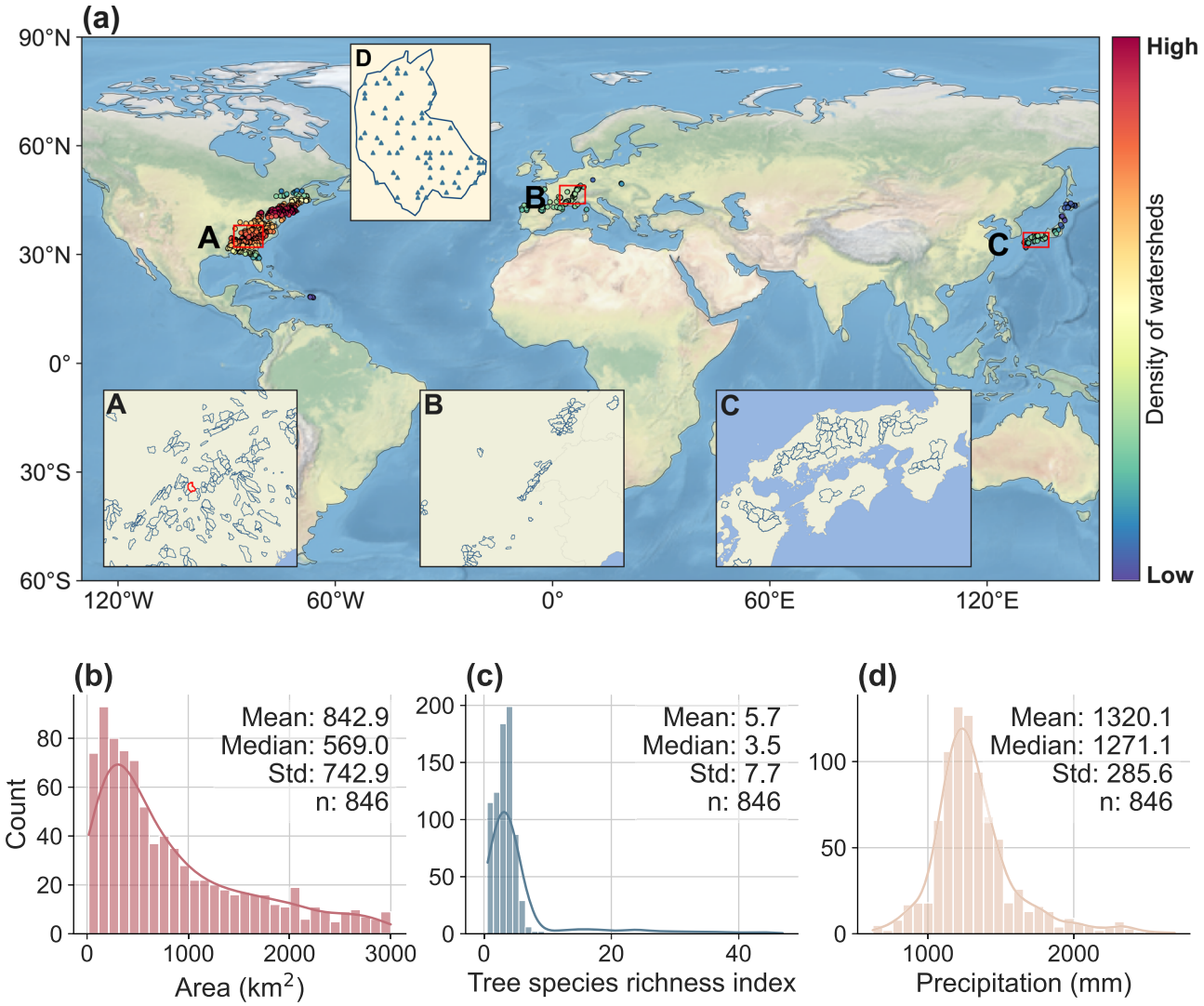

Fig. 1 | Spatial distribution and environmental conditions of watershed samples in this study are based on 846 watershed samples. a Global distribution and spatial density of watershed samples. Boxes A, B, and C are local enlargements, and Box D shows a specific watershed sample (shown in red boundary in Box A) with the spatial distribution of forest plots within it. Histograms of **b** watershed area, **c** quadrat-based tree species richness index, and **d** precipitation distribution. The base world map in (**a**) is from a free-access public map dataset, Natural Earth, www.naturalearthdata.com. Source data are provided as a Source data file.

significant positive correlation between tree species richness and watershed ecological multifunctionality across all calculation indices (Figs. 2a and 3a, b) after controlling for other influencing factors. In the context of watersheds, we propose that high tree species richness likely contributes to the formation of heterogeneous microenvironments and mosaic habitats[31]. These diverse biological structures may support a wide range of ecological functions by maintaining diverse microclimates[32], soil conditions[33], and hydrological regimes[34]. Consequently, this expanded spatiotemporal niche space may allow diverse plant communities to maximize resource capture and functional distinctiveness through complementary interactions across the watershed[35]. Therefore, tree species richness appears to serve as a critical driver promoting the aggregate ecological multifunctionality of watersheds.

In addition to the independent and direct influence of tree species richness, the concurrent positive associations between richness, canopy cover, and multifunctionality imply a potential mechanistic pathway where forest structural attributes may act as important links between biodiversity and watershed ecological multifunctionality (Fig. 3). Higher tree species richness potentially promotes more efficient canopy packing and vertical stratification[36,37], which might contribute to the increased canopy cover observed in our study. Such a dense and structurally complex canopy may, in turn, enhance critical ecosystem fluxes—including rainfall interception, transpiration, and carbon assimilation[36,38] by promoting complementary resource utilization among species through spatial, physiological, and temporal differentiation[37]—thereby promoting ecological multifunctionality. Our exploratory mediation analysis quantitatively confirmed these potential influence pathways, revealing that the indirect effects of species richness mediated through canopy cover are positive and significant (Tables S8, S9, and Fig. S11). Notably, the magnitude of these indirect effects is equivalent to 32% of the direct effects for both the mean-based and PCA-based multifunctionality indices. Nevertheless, there is potential for bidirectional feedback between tree species richness and forest structural attributes, as heterogeneous forest structures may in turn influence tree species richness by altering the local environment[39].

Climatic factors predominantly drove variation in watershed ecological multifunctionality and collectively accounted for nearly half of the total relative importance across multifunctionality indices. Precipitation was the most influential climate factor (Fig. 3). In comparison, soil and topographic factors had a smaller impact on

https://doi.org/10.1038/s41467-026-74914-z

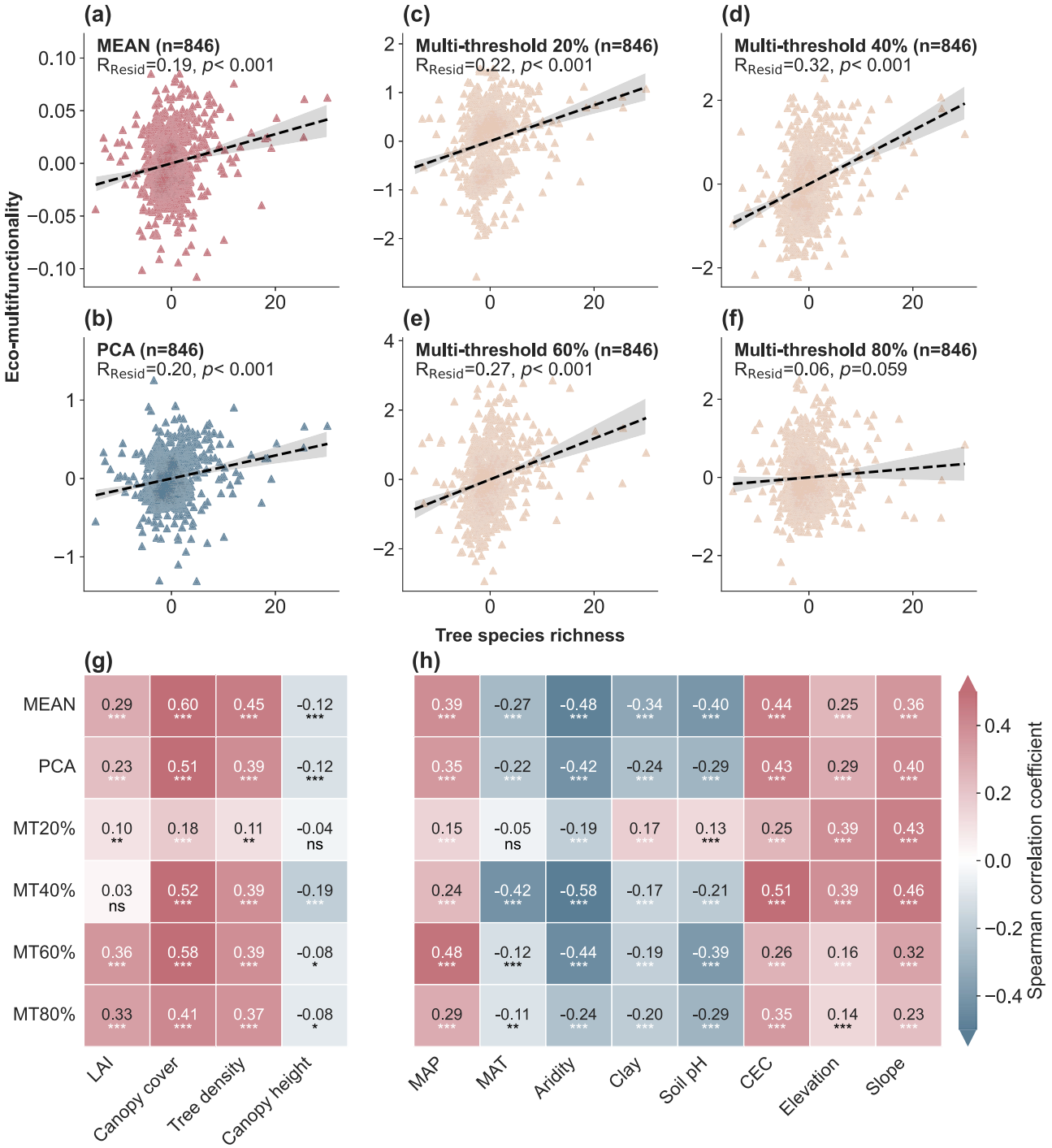

Fig. 2 | Relationships between tree species richness, forest structure, environmental drivers, and ecosystem multifunctionality (EMF) based on 846 watershed samples. Scatter plots show partial residual relationships between tree species richness and EMF indices after controlling for other predictors, including **a** mean-based, **b** PCA-based EMF indices, and multi-threshold-based EMF indices at **c** 20%, **d** 40%, **e** 60%, **f** 80% thresholds, respectively. The residuals were calculated by controlling for other forest structural, climatic, soil, and topographic variables. Displayed solid lines represent fitted linear regression lines, and shaded areas indicate 95% confidence intervals, with Spearman correlation coefficients (R_{resid}) labeled. Heatmap of Spearman correlation coefficients between EMF indices (rows) and potential predictors (columns), shown separately for **g** forest structural attributes (LAI, canopy cover, tree density, canopy height) and **h** environmental factors (climate, soil, and topography). Significance levels in (**g**, **h**): * $p < 0.05$, ** $p < 0.01$, and *** $p < 0.001$, exact p-values are provided in the Source data file. Statistical relationships for all panels were assessed using two-sided Spearman correlation tests. All source data are provided as a Source data file.

multifunctionality (Figs. 3, S6–S8, and Tables S4, S5). In addition, to test the robustness of our results, we also accounted for atmospheric nitrogen deposition in a subset of watersheds where data were available[40]. The results showed that nitrogen deposition had limited explanatory power and did not alter the observed relationship between tree species richness and multifunctionality (Fig. S12).

Additionally, the diminishing effect of species richness at high thresholds (e.g., >70%) is expected and may reflect the inherent physiological and physical trade-offs among ecosystem functions. While biodiversity enhances the overall capacity of ecosystems to sustain multiple functions at moderate levels, it is constrained by trade-offs from simultaneously maximizing all functions to extreme levels.

https://doi.org/10.1038/s41467-026-74914-z

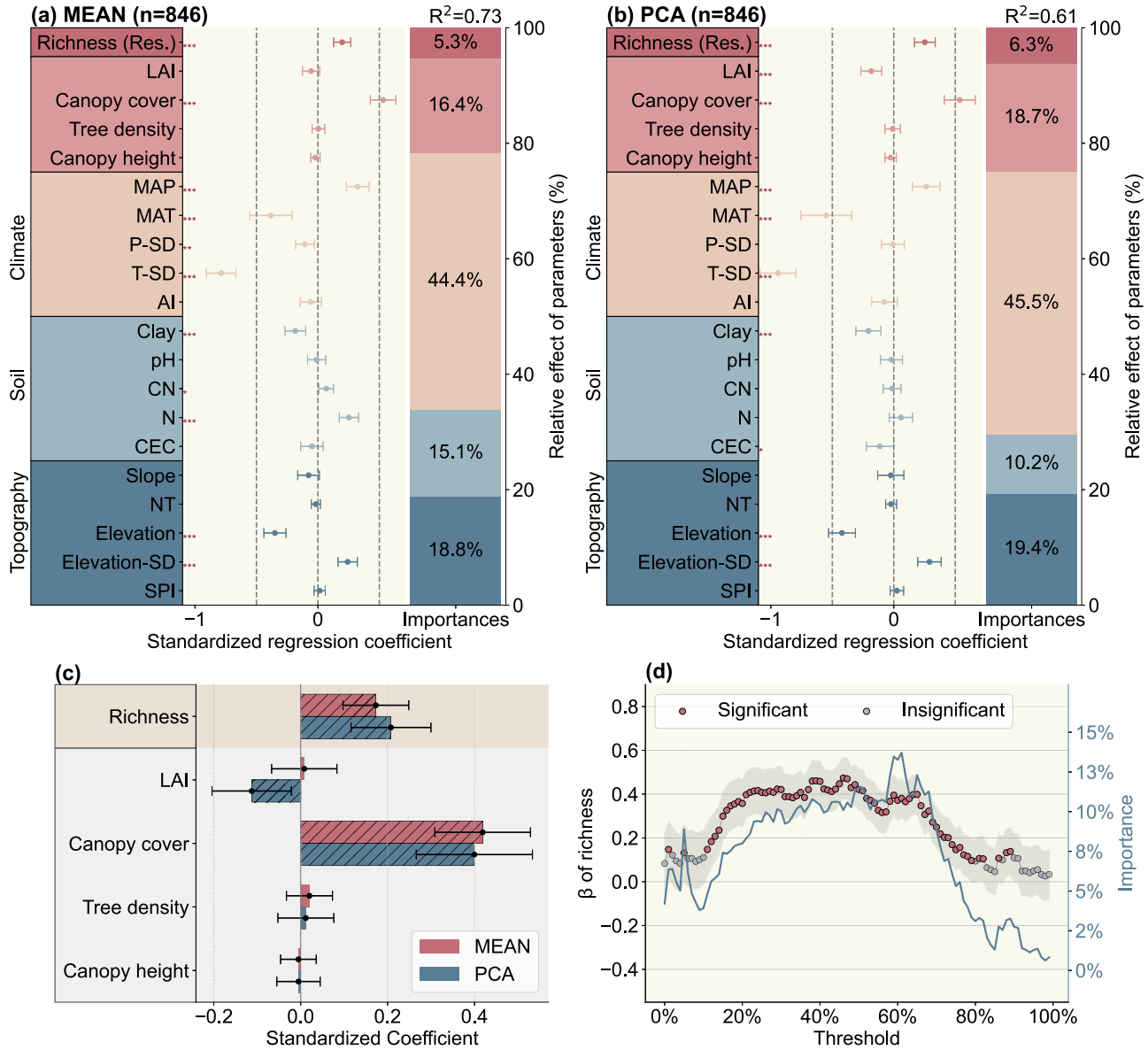

Fig. 3 | Drivers of ecosystem multifunctionality (EMF) based on 846 watershed samples. Standardized ordinary least squares (OLS) regression coefficients of biotic and abiotic predictors for EMF calculated using **a** the mean-based method (MEAN) and **b** the principal component analysis (PCA) method. Bars represent point estimates of standardized regression coefficients from regression models, and error bars indicate 95% confidence intervals. (significance levels: * $p < 0.05$, ** $p < 0.01$, and *** $p < 0.001$, exact p values for each predictor are provided in the Source data file). Richness (Res.) in (**a**, **b**) denotes the statistically residualized tree species richness used to isolate the independent contribution of richness, obtained by regressing richness against all other predictors. Stacked bars show the relative importance of each predictor category in the OLS models. **c** Standardized Ridge regression coefficients showing the effects of species richness and four forest structural attributes (LAI, canopy cover, tree density, and canopy height) on MEAN and PCA EMF. Bars represent point estimates, error bars indicate 95% confidence intervals, and hatched bars denote significant effects ($p < 0.05$). Exact p-values and confidence intervals are provided in the Source data file. **d** Sensitivity analysis of the effect of species richness on multi-threshold EMF across thresholds from 1 to 99%. Red points indicate standardized OLS regression coefficients (β) of species richness, and the blue line indicates the relative importance of species richness. Shaded areas indicate 95% confidence intervals. Colored and grey points indicate significant and nonsignificant relationships, respectively. Statistical significance in (**a**, **b**, **d**) was assessed using two-sided t-tests for regression coefficients, whereas significance in (**c**) was assessed using two-sided bootstrap tests. LAI leaf area index, MAP mean annual precipitation, MAT mean annual temperature, P-SD standard deviation of monthly precipitation, T-SD standard deviation of monthly temperature, AI aridity index, CN carbon to nitrogen ratio, N nitrogen content, CEC cation exchange capacity, NT northness, SPI stream power index, Elev. elevation. See Table S2 for predictor details and Tables S4 and S5 for OLS model outputs. All source data are provided as a Source data file.

Additionally, this pattern aligns with the mathematical property of the multi-threshold approach, where the variance in multifunctionality scores naturally decreases at higher thresholds, limiting the detectability of biodiversity effects.

We recognize inherent limitations of this study, particularly regarding the challenges of large-scale data integration and the scope of spatial extrapolation. First, while our results demonstrate a consistent positive relationship between tree species richness and multifunctionality across temperate and subtropical watersheds, caution is warranted when extrapolating these findings to biomes with fundamentally different environmental constraints, like boreal forests (limited by temperature) or tropical forests. Second, we acknowledge that certain functional proxies, such as soil organic carbon, gross primary productivity, and evapotranspiration, represent modeled spatial

distributions rather than dense networks of in situ soil measurements, although they facilitate large-scale macroecological synthesis. This inherent characteristic implies that shared variance between model predictors and tree richness may potentially cause observed relationships to partially reflect the underlying data-generation properties. Nevertheless, these datasets (e.g., SoilGrids, MOD17A3HGF, and MOD16A2GF) did not use the tree richness index as an input variable during production. We believe these impacts are effectively mitigated in our study by employing a stringent residual-based approach to isolate the biodiversity signal from environmental or structural proxies. Moreover, most functional proxies used in our study were obtained from in-situ observation or remote sensing products (Table S1). The sensitivity analysis by sequentially removing each functional proxy further indicates that the positive correlation between tree richness and multifunctionality is robust, and our core conclusions still hold (Tables S14 and S15). In the future study, leveraging the increasing availability of open-source watershed data and expanded in situ observations in currently underrepresented regions will be essential in addressing geographical and data-specific constraints, thus, could further test the robustness and generality of our findings.

In addition, we note that the tree species richness metric used in this study is a plot-based richness index derived from spatially referenced forest inventory plots, rather than a total species count aggregated across entire watersheds. In the future, LiDAR-based remote sensing of forest tree diversity may help characterize tree species richness across entire watersheds, thereby providing a complementary richness dimension at the basin scale. Integrating such data could help test whether the observed richness-multifunctionality relationship remains consistent across different tree diversity characterizations.

Effects of tree species richness on individual ecological functions of the watershed

The analysis of individual ecological functions revealed distinct roles for tree species richness and forest structural attributes (Fig. 4 and Tables S10–S13). Specifically, while controlling for other influential factors, richness was a strong positive driver of net carbon accumulation rate in tree stem (standardized $\beta = 0.27$, 95% CI = 0.15–0.39, $t(825) = 4.45$, $p < 0.001$) and hydrology-related metrics, such as soil moisture (standardized $\beta = 0.35$, 95% CI = 0.26–0.44, $t(825) = 7.65$, $p < 0.001$), flood control (standardized $\beta = 0.17$, 95% CI = 0.06–0.28, $t(825) = 2.95$, $p = 0.003$), and minimum water supply capacity (standardized $\beta = 0.26$, 95% CI = 0.14–0.38, $t(825) = 4.15$, $p < 0.001$) (Fig. 4d and Tables S10, S11).

Canopy cover fraction emerged as the primary determinant of biomass carbon storage (standardized $\beta = 0.89$, 95% CI = 0.78–1.00, $t(825) = 15.93$, $p < 0.001$), while simultaneously enhancing runoff stability (standardized $\beta = 0.19$, 95% CI = 0.01–0.38, $t(825) = 2.03$, $p = 0.043$) and soil stability (standardized $\beta = 0.26$, 95% CI = 0.14–0.38, $t(825) = 4.15$, $p < 0.001$) (Fig. 4e and Tables S10, S12). In contrast, for forest structural attributes, such as LAI, tree density and canopy height, the divergent positive and negative effects on individual functions tended to counterbalance each other, resulting in a negligible or weak overall influence on multifunctionality (Figs. 4f and S9, Tables S10, S13).

Our analysis of individual ecological functions revealed that although tree species richness and canopy cover fraction induced trade-offs among individual functions, their cumulative positive effects outnumbered and statistically exceeded the negative associations within the scope of the functions we assessed. This resulted in a predominantly positive contribution to the observed watershed ecological multifunctionality (Fig. 4 and Tables S10–S13). Crucially, forest structural attributes played specific roles that complemented biodiversity, especially on carbon stocks (biomass storage) as well as runoff stability and soil control (Fig. 4b, d). We propose that tree species richness may facilitate greater canopy cover, which in turn enhances carbon storage and drives specific ecological functions that richness alone cannot support. This finding is highly aligned with the latest experimental study, which reported that increased canopy structural complexity of forest consistently explains the positive effects of tree diversity on productivity[36].

Forest tree species richness index had significant relationships with some water-related functions, especially water supply and soil water retention, even under the significant influence of climate factors on ecological functions (Fig. 4a, d, and Table S9). Diverse tree species compositions may lead to greater root richness and density, increasing soil porosity and structural stability[41], which can promote rainwater infiltration and soil moisture retention[42]. Additionally, diverse tree species compositions may create complementary water resource utilization regimes at the watershed scale[43], thereby enhancing forest resilience during droughts[5].

Our analysis of individual ecological functions revealed that tree species richness was positively associated with the net carbon accumulation rate (Fig. 4d). This aligns with findings of Liang et al.[9], who explored the relationship between forest tree species richness and carbon sequestration with the same dataset. Furthermore, our results establish a significant positive relationship between tree species richness and long-term carbon storage pools, including both biomass and SOC (Fig. 4d). This broad-scale observation aligns with extensive empirical evidence suggesting that tree diversity is positively associated with ecosystem carbon storage and forest biomass across diverse climatic gradients[44–46]. The potential enhancement of these carbon-related functions by tree diversity is often attributed to ecological niche complementarity and selection effects[46]. Diverse tree communities likely utilize available resources more efficiently through spatial and temporal niche partitioning[47]. This resource optimization could be driven by stronger complementarity in functional traits—such as shade tolerance and growth strategies—which in turn may bolster stand-level biomass production across various forest biomes[48].

Scale and climatic dependency of tree species richness-watershed ecological multifunctionality relationships

To explore the climatic and spatial scale dependencies of the effects of tree species richness index and forest structural characteristics on multifunctionality, we employed a moving window approach to quantify how the strength of these effects varies with watershed area and climatic factors (Figs. 5 and S10). The window was advanced across the watershed samples, reordered by watershed area or climatic factors, generating adjacent sampling subsets to estimate the influences of forest tree species richness index and structural characteristics on multifunctionality. The strengths of these effects were estimated using Spearman correlation coefficients between tree species richness index (or canopy cover fraction, or LAI) and multifunctionality. We found that the Spearman correlation between various multifunctionality indices and the tree species richness index significantly increased with watershed area (Figs. 5a and S10). In addition, the results were almost identical for 100 and 50 window sizes, suggesting the analysis are robust to the window sizes. In contrast, there was no consistent spatial scale dependency for the Spearman correlation between multifunctionality indices and LAI (Fig. 5d), as well as canopy cover fraction (Fig. 5c). Previous studies have also indicated that factors influencing the BEF relationship are affected by spatial scale[15,49–51]. We infer that the underlying mechanisms may include, firstly, larger watersheds encompassing different microclimates[32], soil types[33], and terrains, which support a variety of tree species adapted to different conditions. This enhances β-diversity and niche differentiation[52], thereby improving resource use efficiency[49,53]. Secondly, at the watershed scale, hydrologically related ecological functions may exhibit spatial cumulative effects[23], thereby enhancing multifunctionality. Tree species richness influences local hydrological characteristics by enhancing

https://doi.org/10.1038/s41467-026-74914-z

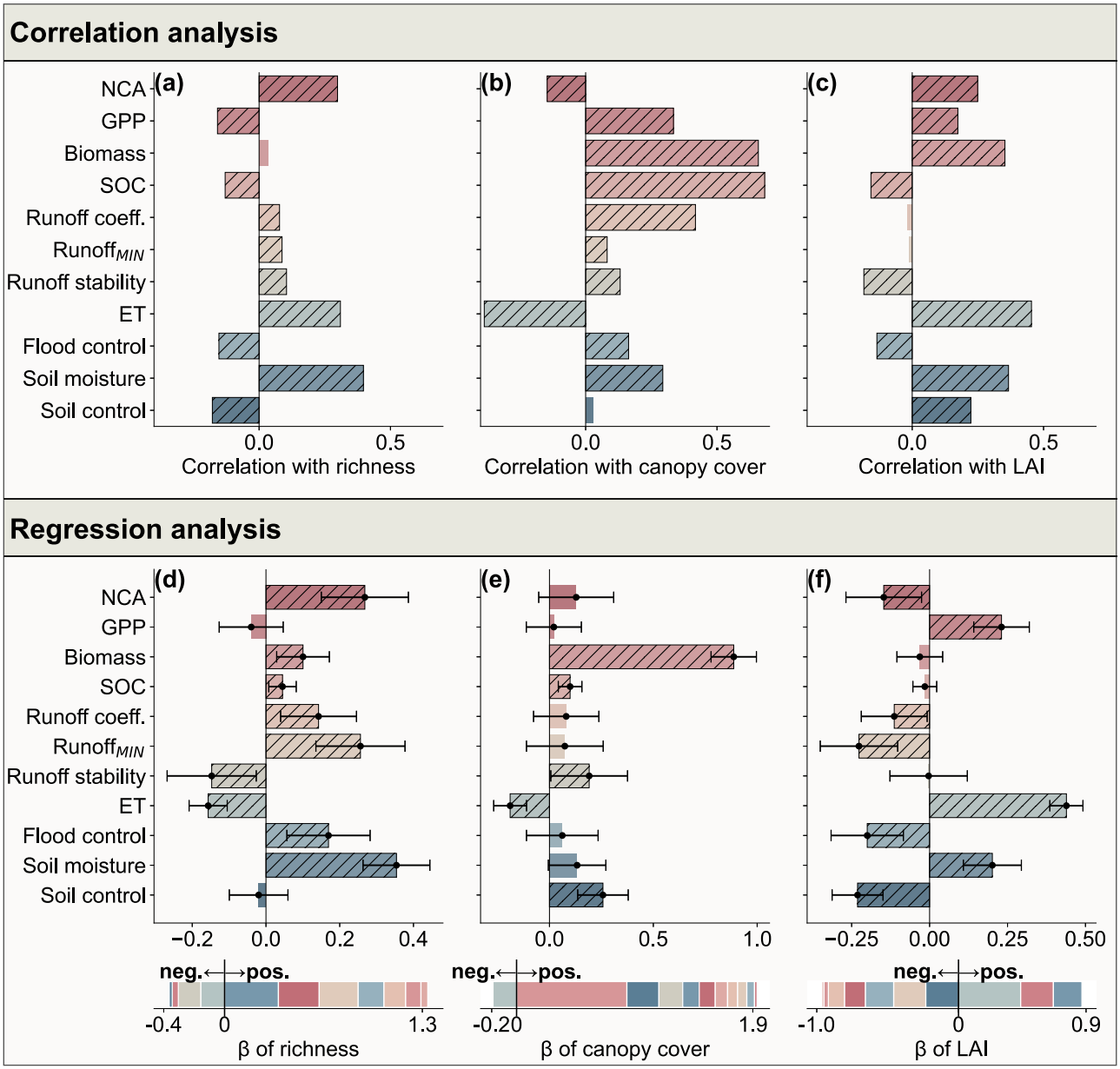

Fig. 4 | Relationships between tree species richness, canopy cover fraction, leaf area index (LAI), and individual watershed ecological functions based on 846 watershed samples. Correlation coefficients between individual ecological functions and **a** species richness, **b** canopy cover fraction, **c** leaf area index (LAI). Standardized ordinary least squares (OLS) regression coefficients of **d** species richness, **e** canopy cover fraction and **f** LAI on individual ecological functions controlling for other environmental variables. Bars represent point estimates of standardized regression coefficients from OLS regression models, and error bars represent 95% confidence intervals in (**d**–**f**). Statistical significance was assessed using two-sided t-tests for regression coefficients. The panels below the regression plots display the aggregated positive and negative effects, calculated by summing the respective regression coefficients. Hatched bars indicate statistically significant relationships ($p < 0.05$), while exact p values are provided in the Source data file. NCA net carbon accumulation rate in tree stem, GPP gross primary productivity, SOC soil organic carbon, ET evapotranspiration, CV coefficient of variation. All source data are provided as a Source data file.

soil structure and increasing water infiltration[54]. These changes in hydrological characteristics are transmitted downstream through hydrological connectivity, eventually converging at the watershed outlet. Therefore, hydrological measurements observed at the river outlet reflect not just a simple average of the entire watershed but rather a spatial accumulation of tree species richness effects. Thus, larger watersheds exhibit a stronger relationship between tree species richness and multifunctionality.

The relationship between the tree species richness index and multifunctionality also depended on climatic context. The results indicate that the correlation between tree species richness index and multifunctionality decreases with the aridity index (Fig. 5b). Additionally, in relatively dry environments, this relationship showed a negative correlation (Fig. 5b). One possible explanation is that under relatively humid climate conditions, water and other resource abundance reduce competition pressure among tree species. This may allow tree species with different functional strategies, such as contrasting photosynthetic characteristics and rooting depths, thereby enhancing overall ecological function[55]. In contrast, in relatively drier conditions, increased water limitation may impose stronger environmental filtering, constrain the functional breadth of co-occurring species, and intensify competition for water, thereby reducing the potential for species richness to enhance ecological functions[56,57,58]. Further research, supported by more open-access data, is needed to

https://doi.org/10.1038/s41467-026-74914-z

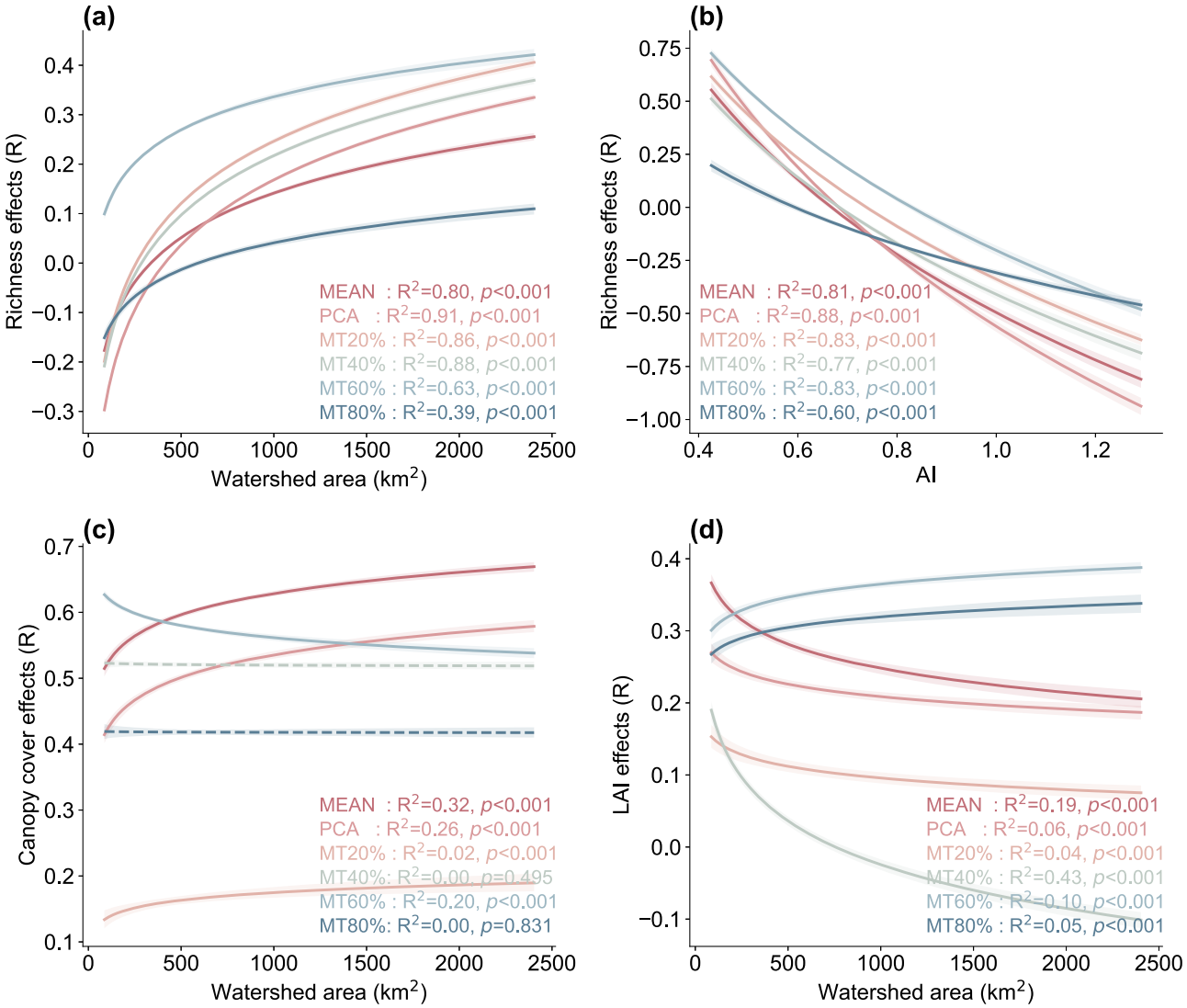

Fig. 5 | Environmental and spatial scale dependencies of the effects of tree species richness index and forest structural characteristics on watershed ecological multifunctionality (EMF) based on 846 watershed samples using a moving-window approach. a The variation of the effects of the quadrat-based tree species richness index on EMF indices across watershed areas. **b** The variation of the effects of tree species richness index on EMF indices across the aridity index (AI) gradient. The variation of the effects of canopy cover fraction (**c**) and LAI (**d**) on EMF indices across watershed areas based on window sizes of 100 watershed samples. All fitted curves are accompanied by associated 95% confidence intervals. For each moving-window estimate, the analysis was based on 100 watershed samples. Curves represent fitted trends of correlation coefficients for each moving window, and shaded areas indicate 95% confidence intervals around the fitted trends. Exact *p*-values for the correlation of each moving window are provided in the Source data file. All source data are provided as a Source data file.

explore the mechanisms underlying the climate-dependency of biodiversity-multifunctionality relationships in watersheds.

Implications for forest and watershed management

To the best of our knowledge, the present study provides a comprehensive understanding of the impacts of the forest tree species richness on watershed multifunctionality. We found that the ecological multifunctionality of watersheds increased significantly with the tree species richness index after controlling for various other influencing factors (Figs. 2 and 3). The cumulative positive impacts of tree species richness were more prevalent among the evaluated individual functions than the negative associations (Fig. 4). This suggests a predominantly positive contribution to the measured dimensions of watershed multifunctionality, although we acknowledge that unmeasured functions could potentially harbor different trade-offs. The implications of this study are significant for forest and watershed management. The positive linkage of tree species richness with watershed ecological multifunctionality suggests that maintaining or enhancing biodiversity can improve critical ecosystem services, especially water regulation. Crucially, our findings advocate for a shift from local ecological protection within isolated stands to watershed-level conservation strategies. Due to their clear natural boundaries for the flow of water and nutrients, watersheds are key units for ecological planning and policy implementation. Ecological protection strategies grounded in the watershed scale should aim to enhance watershed multifunctionality. Finally, the study emphasizes the importance of climate in driving watershed multifunctionality, suggesting that conservation and management practices should be adapted to local climate conditions, particularly in regions with varying humidity levels. This research encourages a shift towards integrating biodiversity with climate-adaptive strategies in forest and watershed management.

Methods

Forest plot data and in situ-based hydrological indices

Forest tree species richness data were derived from the Global Forest Biodiversity Initiative (GFBI) dataset, which is comprised of ground-

sourced forest inventory data from 777,126 permanent forest plots in 44 countries containing more than 30 million trees from 8737 species spanning most of the global terrestrial biomes[9]. The data used here were standardized and harmonized from individual tree-level field records from multiple national forest inventory and private forest inventory datasets, using a data cleaning and standardizing protocol introduced in Liang et al.[59]. Intensively managed forests with harvests exceeding 50 percent of the stocking volume were excluded from this dataset.

Hydrological indices data were derived from the Global Streamflow Indices and Metadata (GSIM) dataset, which collated publicly available data (seven national databases and five international collections), applied basic consistency to the formatting, and established a standardized set of metadata[29,30]. GSIM is a worldwide collection of metadata and indices derived from more than 35,000 daily streamflow time series[29,30]. The dataset provides a set of quality-controlled time-series indices representing the water balance, the seasonal cycle, low flows, and floods. The dataset also contains vector boundaries for each watershed.

Watershed selection

We filtered suitable watersheds from the GSIM dataset to select the study samples based on data availability and comparability. We spatially matched the GFBI forest plot dataset with the watershed boundaries of the GSIM hydrological dataset, retaining only watersheds with at least five forest plots and a minimum density of one forest plot per 100 km^2. Then, we meticulously selected watersheds with hydrological observations based on a series of key criteria before conducting the analysis. First, we limited watershed areas to below 3000 km^2, which is about the average area of watersheds at a medium level (level seven) based on the hydrosheds watershed delineation product[60], as larger sizes introduce more uncertainty. Second, each watershed needs to have a sample density of at least one plot per 50 km^2. In the third step, we selected watersheds primarily covered by forests. According to the definitions employed by the UN Framework Convention on Climate Change (the Kyoto Protocol), an area is considered forested if more than 30% of the land ($\geq$ 0.5 ha) is covered with trees. We adopted stricter criteria to analyze forest cover on the Google Earth Engine platform using two datasets: the Hansen Global Forest dataset[61] and the MODIS land cover dataset (MCD12Q1 version 061)[62]. We retained watersheds where the average canopy cover fraction exceeds 50% for each watershed from 2000 to 2012, and the percentage of forest (tree canopy cover > 60%) and woody savanna (tree canopy cover between 30 and 60%) in the MODIS land cover classification exceeds 70%. Additionally, watersheds should have hydrological observation records of over 10 years post-1980, ensuring that the data collected is both extensive and contemporary. We considered years with at least 330 observation days as valid for our analysis. Lastly, we assessed the distribution of forest plots within the watersheds to ensure they were representative by conducting topological analysis and generating convex hulls for the forest plots. If the convex hull area exceeded 70% of the total watershed area, the forest plots were deemed adequately representative of the overall forest conditions within the watersheds.

Using stringent selection criteria as outlined above, we identified 846 forest watersheds from the datasets (Fig. 1a), containing 55,337 spatially referenced forest plots within these watersheds. These samples are mainly located between 30°N and 45°N in North America, Europe, and Japan (Fig. 1a). Over 60% of these watersheds have areas smaller than 1000 km^2 (Fig. 1b) and quadrat-based tree species richness index below eight (Fig. 1c). On average, there are 65 forest plots per watershed, with a density of 1 forest plot per 13.9 km^2 (Fig. S1). The climate in these watersheds is generally humid, with a mean precipitation of 1320.1 mm and an average temperature of 11.9 °C, characteristic of subtropical or temperate climate zones (Figs. 1d and S2). The average elevation of the watershed samples is 419.8 m, with 85% below 700 m (Fig. S2).

Ecological functions of watersheds

Using the GFBI forest plot dataset, GSIM hydrological dataset, and other global datasets, we calculated watershed ecological multifunctionality (EMF) indices by obtaining representative variables for various ecological functions. We selected five major categories (11 independent measurements) of watershed functions: carbon sequestration, carbon storage, water supply, water regulation, and soil conservation (Table S1). For the proxy indicators that are inversely associated with ecological functions, we used their additive inverse to replace them.

Carbon sequestration functions include metrics that measure the ability of ecosystems to assimilate and accumulate carbon. Net carbon accumulation rate is assessed through the periodic annual increment in stem volume, derived from the GFBI forest plot dataset. The carbon assimilation rate is quantified by the annual gross primary productivity, derived from Moderate-Resolution Imaging Spectroradiometer (MODIS) MOD17A3HGF[63] with a spatial resolution of 500 m × 500 m. Carbon storage functions include metrics that measure the amount of organic carbon long-term accumulated. Biomass carbon storage encompasses both above and below-ground biomass carbon, measured in tons per square kilometer (t/km^2), derived from Global Aboveground and Belowground Biomass Carbon Density Maps from NASA Oak Ridge National Laboratory[64] with spatial resolution of 300 m × 300 m. Soil organic carbon content, also in tons per square kilometer (t/km^2), was derived from the SoilGrid dataset (https://soilgrids.org/)[65].

Water supply functions focus on the availability and reliability of water resources. The runoff coefficient, defined as the ratio of annual total runoff to total precipitation, illustrates the proportion of rainfall that is available in the streams. Precipitation was from the TerraClimate dataset[66] with a spatial resolution of 4 km × 4 km. Relative minimum water supply capacity is measured by the ratio of the average flow of the 7 lowest flow days (mm/d) to annual mean streamflow (mm/d), providing insight into water availability during dry periods. Water supply stability is evaluated by the additive inverse of the standard deviation of daily runoff (mm/d), indicating the variability and predictability of water supply. All these streamflow-related indicators were derived from the GSIM dataset.

Water regulation functions pertain to the processes that control water distribution and movement. The annual total evapotranspiration is measured in millimeters per year (mm/yr), derived from MOD16A2GF datasets[67] with a spatial resolution of 500 m × 500 m. Flood control function was measured by the additive inverse of the ratio of the average flow of the 7 highest flow days (mm/d) to annual mean streamflow (mm/d), which helps assess the potential for flood control. Surface soil water content, measured as the annual average surface soil water content (m^3/m^3), from a remote-sensing-based surface soil moisture dataset[68] with spatial resolution of 0.1° × 0.1°.

Soil conservation function focuses on soil stability and its susceptibility to erosion. Soil stability was assessed through the additive inverse of the soil erodibility factor, which reflects the potential for soil to be eroded based on its properties. The soil erodibility factor was from the advanced global soil erodibility map[69] with a spatial resolution of 1 km × 1 km.

We derived the mean of variables at the watershed scale based on these global datasets. Forest biomass data and precipitation data were processed on the GEE platform and derived using the "geemap" (version 0.36) Python package[70]. Other data were downloaded from associated links and processed with Python 3.11. The average values of all available data from 2000 to 2020 of these datasets were used as individual ecological functions for each watershed. Finally, a collinearity test was performed on all functional variable proxies, which revealed a maximum correlation coefficient of 0.53 (Fig. S3). Details about data sources can be found in Table S3.

Watershed ecological multifunctionality indices

Based on the aforementioned ecological function variables, we calculated the ecological multifunctionality (EMF) indices at the watershed scale using three independent methods which have frequently been employed to measure EMF in recent literature[71–74]: mean-based EMF indices, principal component analysis-based (PCA-based) EMF indices, and multi-threshold EMF indices. The three independent methods each have unique characteristics. Mean-based EMF indices provide an intuitively interpretable measure of a watershed's ability to deliver multiple functions. PCA-based EMF indices can eliminate uncertainties caused by potential collinearity among functions. However, these two types of EMF indices ignore potential trade-offs among functions and assume substitutability among functions[75,76], which is an issue addressed by multi-threshold EMF indices. By combining these three EMF indices, we achieved a comprehensive assessment of EMF.

Before calculation, all individual ecological function proxy indicators were normalized by a "min-max" normalization approach to transform all indicators within a range of 0–1[74]. To calculate mean-based EMF indices, we computed the average of all ecological functions. Using this method, we also calculated EMF indices for individual function groups: carbon sequestration, water supply, water regulation, and soil conservation. For PCA-based EMF indices, we employed PCA, then calculated the weighted sum of the leading principal components that collectively explained over 80% of the total variance. The PCA-based approach minimizes multicollinearity among ecological functions. Multi-threshold-based EMF was defined as the number of ecological functions of a watershed that had a value above a threshold. Threshold values were defined as a certain integer percentage of maximum functioning. EMF was systematically calculated for all integer threshold levels from 1 to 99%[75]. Following the recommendation as described in ref. 75, we determined the maximum level of functioning as the average of the top 5% values measured for the respective function among all watersheds.

Predictors of watershed multifunctionality

To explore the influencing factors of EMF, we selected a variety of forest characteristics factors and environmental factors as predictors of EMF (Table S2). Forest characteristics include tree species richness and forest structure indicators. Tree species richness is measured by an index that is the weighted average of the quadrat-based number of tree species in each watershed. Forest structure indicators include leaf area, canopy cover fraction, tree density, and canopy height. Leaf area is indicated by the leaf area index (LAI), representing the leaf area per unit area of the watershed. Canopy cover fraction is the vertical projection of the canopy elements of forests in a watershed onto the ground surface, expressed as a percentage of the total forest area. Tree density is assessed by the number of trees per square kilometer in the watershed. Canopy height is represented by the average height of the forest canopy in meters over the watershed.

Environmental factors encompassed climatic conditions, soil properties, and topographical features. Climate factors cover key indicators that affect ecological functions. Precipitation is measured by the annual total precipitation in millimeters. Temperature is represented by the annual average temperature in degrees Celsius. Precipitation seasonality is indicated by the standard deviation of monthly average precipitation in millimeters, while temperature seasonality is measured by the standard deviation of monthly average temperature in degrees Celsius. The aridity index, which is the ratio of annual precipitation to annual potential evapotranspiration, reflects the dryness of the watershed. To obtain the most representative predictors and avoid multicollinearity among these variables, we used a backward stepwise regression method to select soil property and topography parameters. From 10 soil property parameters and 12 topography parameters, this method selected the five most important parameters from each group to serve as EMF predictors (Table S2). Soil factors are characterized by a number of biophysical and biogeochemical measures, including percent of clay, soil pH, C/N ratio, total soil N content, and cation exchange capacity. Topography factors encompass indicators related to the physical landscape of the watershed. Slope is measured as the average slope percentage of the watershed. Northness is represented by the northness index, ranging from −1 to 1, where a value close to −1 corresponds to a steep southern slope with high solar exposure. Elevation is indicated by the average elevation in meters above the mean sea level, while elevation variation is represented by the standard deviation of elevation within the watershed. The stream power index is a dimensionless measure reflecting the erosive power of water flow and the influence of gravitational forces on water movement downstream.

The quadrat-based tree species richness index was derived from GFBI forest plots[9]. We applied kriging interpolation to the forest sampling plots within each watershed to obtain spatial raster data for the number of tree species. Based on this, we calculated the average forest tree species richness index for each watershed. LAI data were obtained from the MODIS MOD15A2H dataset (version 061)[77] with a spatial resolution of 500 m × 500 m. Canopy cover fraction was from the MODIS MOD44B dataset (version 061)[78] with a spatial resolution of 250 m × 250 m. Tree density data came from a published forest tree density map[79] with spatial resolution of 1 km × 1 km, while canopy height data were sourced from the published forest extent and height change dataset[80] with spatial resolution of 30 m × 30 m. Climatic variables were derived from the TerraClimate dataset with a spatial resolution of 4 km × 4 km. Soil properties were obtained from the SoilGrid dataset (https://soilgrids.org/)[65] with a spatial resolution of 250 m × 250 m. Topography parameters were sourced from the multi-error-removed improved terrain (MERIT) digital elevation model (DEM)[81] and the Geomorpho90m dataset, which includes various terrain parameters generated from the MERIT DEM[82] with a spatial resolution of 90 m × 90 m. All these spatial datasets (except for tree density) were processed on the GEE platform, and statistics were calculated using the "geemap" (version 0.36) Python package[70]. Tree density data were downloaded locally from associated links and processed with Python 3.11. The average values of all available data from 2000 to 2020 of these datasets were used as EMF predictors for each watershed. Details about data sources can be found in Table S3.

Statistical analysis

We first conducted binary OLS regression and Spearman correlation between forest tree species richness index and averaging-based EMF indices, PCA-based EMF indices, and multi-threshold EMF indices (EMF_{MT}), as well as individual ecological functions. To further evaluate the independent effect of tree species richness while accounting for confounding factors, we employed partial correlation analysis and partial regression plots. In this approach, we correlated the residuals of richness (obtained by regressing it against all other biotic and abiotic covariates) with the residuals of the EMF indices, providing a decoupled view of the biodiversity-multifunctionality link. We also estimated relationships between forest structural characteristics (i.e., LAI, canopy cover fraction, tree density, and canopy height) and these EMF indices.

We employed multiple OLS regression models to assess the combined effects of forest tree species richness index, forest structural characteristics (i.e., LAI, canopy cover fraction, tree density, and canopy height), and environmental factors (i.e., climate, soil, and topography) on various EMF indices, as well as the relative importance of individual variables. To address potential multicollinearity and ensure the stability of our ecological inferences, we implemented a more rigorous residuals-based framework. Specifically, we calculated the "independent" residuals of richness not explained by all other covariates (forest structure, climate, soil, and topography). By incorporating these decoupled residuals into our OLS models, we ensured that the biodiversity signal was mathematically isolated from environmental and structural drivers. Furthermore, we performed Ridge

regression to provide robust coefficient estimates and validate our OLS results under different modeling constraints. Ridge regression is a regularized machine learning technique that is specifically effective at mitigating the effects of multicollinearity. The predictors used in the regression model were detailed in the previous section. Additionally, we included the quadratic term of the forest tree species richness index, as previous research has indicated that biodiversity might influence ecological functions in a nonlinear manner[83]. Before analysis, all predictor and response variables were standardized using z-scores to enable comparable interpretation of parameter estimates. To evaluate the relative importance of forest tree species richness index, forest structural characteristics, and environmental factors as drivers of EMF, we expressed the importance of each predictor group as a percentage of the total effect they explained. This was done by comparing the absolute values of their standardized regression coefficients with the sum of the absolute values of all standardized coefficients. We conducted the OLS and Ridge regression analysis using the "statsmodels" (version 0.14.2) and "scikit-learn" (version 1.7) Python packages.

To investigate the potential mechanisms linking forest tree species richness to ecological multifunctionality, we performed a causal mediation analysis. We examined whether the effects of species richness on EMF indices (i.e., mean-based and PCA-based indices) were mediated by forest structural attributes, specifically LAI, canopy cover, tree density, and canopy height. The analysis involved estimating two regression models for each potential mediator: (1) a mediator model, which predicted the forest structural variable based on species richness, and (2) an outcome model, which predicted the EMF index based on both tree species richness and the mediator. To ensure the robustness of the mediation effects, we included environmental factors (climate, soil, and topography), the quadratic term of species richness, and other forest structural variables as covariates in all models. The average causal mediation effect was estimated using the "mediation" class within the "statsmodels" (version 0.14.2) Python package. Significance levels and 95% confidence intervals for the indirect effects were determined using a simulation-based approach with 500 replications.

We applied a moving window approach to explore the scale and climatic dependency of the relationship between the tree species richness index and EMF. This method helped to understand how the impact of the tree species richness index on EMF varies along a gradient of another variable. We examined the scale dependency by analyzing the trend of the relationship between the tree species richness index and EMF across watershed areas. Additionally, we explored this relationship along gradients of a significant climatic variable (aridity index). Specifically, we first sorted all data by watershed area (or aridity index) in ascending order. Then, we moved the window across watershed samples to generate adjacent watershed subsets. Then, the Spearman correlation coefficients between the tree species richness index and EMF were calculated for each watershed subset as a proxy of the effects of tree species richness on EMF. To mitigate the potential impact of window size on the results, we used window sizes of 100 and 50 watersheds for sampling. The relationship between the tree species richness index and EMF was represented by the Spearman correlation coefficient. Finally, we used bivariate least squares regression to investigate the trend of the tree species richness index-EMF relationship with changes in area (or environmental variables).

Reporting summary

Further information on research design is available in the Nature Portfolio Reporting Summary linked to this article.

Data availability

The selected watershed samples, their ecological function proxy variables and environmental factors, used for analysis in this study, can be found at https://osf.io/ydgxj/. All display items presented in the main manuscript and supplementary information can be reproduced from raw data and code shared in this public repository. The quadrat-based tree species richness index and forest productivity was derived from Global Forest Biodiversity Initiative (GFBI) forest plots[9], the raw data of which can be obtained through the Science-i cyberinfrastructure (https://science-i.org/). All streamflow-related functions were derived from the Global Streamflow Indices and Metadata (GSIM) dataset[29,30]. Gross primary productivity and evapotranspiration data were from Moderate-Resolution Imaging Spectroradiometer (MODIS) MOD17A3HGF[63] and MOD16A2GF datasets[67] (version 061), respectively. Leaf area index data were obtained from the MODIS MOD15A2H dataset (version 061)[77]. Canopy cover fraction was from the MODIS MOD44B dataset (version 061)[78]. Climatic variables were derived from the TerraClimate dataset[66]. Forest biomass data were from Global Aboveground and Belowground Biomass Carbon Density Maps from NASA Oak Ridge National Laboratory[64]. Soil properties were obtained from the SoilGrid dataset (https://soilgrids.org/)[65]. Soil water content was from a remote-sensing-based surface soil moisture dataset[68]. Soil erodibility factor was from the advanced global soil erodibility map from ref. 69. Tree density data came from a published forest tree density map[79], while canopy height data were sourced from the published forest extent and height change dataset[80]. Topography parameters were sourced from the multi-error-removed improved terrain (MERIT) digital elevation model (DEM)[81] and the Geomorpho90m dataset, which includes various terrain parameters generated from the MERIT DEM[82]. Source data are provided with this paper.

Code availability

The code for the analysis is available for download from https://osf.io/ydgxj/.

References

1. Farooqi, T. J. A. et al. Global progress in climate change and biodiversity conservation research. *Glob. Ecol. Conserv.* **38**, e02272 (2022).
2. Leadley, P. et al. Achieving global biodiversity goals by 2050 requires urgent and integrated actions. *One Earth* **5**, 597–603 (2022).
3. Hisano, M., Ghazoul, J., Chen, X. & Chen, H. Y. H. Functional diversity enhances dryland forest productivity under long-term climate change. *Sci. Adv.* **10**, eadn4152 (2024).
4. Crockett, E. T. H. et al. Structural and species diversity explain aboveground carbon storage in forests across the United States: evidence from GEDI and forest inventory data. *Remote Sens. Environ.* **295**, 113703 (2023).
5. Liu, D., Wang, T., Peñuelas, J. & Piao, S. Drought resistance enhanced by tree species diversity in global forests. *Nat. Geosci.* **15**, 800–804 (2022).
6. Jochum, M. et al. The results of biodiversity–ecosystem functioning experiments are realistic. *Nat. Ecol. Evol.* **4**, 1485–1494 (2020).
7. Gamfeldt, L. & Roger, F. Revisiting the biodiversity–ecosystem multifunctionality relationship. *Nat. Ecol. Evol.* **1**, 1–7 (2017).
8. Duffy, J. E., Godwin, C. M. & Cardinale, B. J. Biodiversity effects in the wild are common and as strong as key drivers of productivity. *Nature* **549**, 261–264 (2017).
9. Liang, J. et al. Positive biodiversity-productivity relationship predominant in global forests. *Science* **354**, aaf8957 (2016).
10. van der Plas, F. Biodiversity and ecosystem functioning in naturally assembled communities. *Biol. Rev.* **94**, 1220–1245 (2019).
11. Delsol, R., Loreau, M. & Haegeman, B. The relationship between the spatial scaling of biodiversity and ecosystem stability. *Glob. Ecol. Biogeogr.* **27**, 439–449 (2018).
12. Gonzalez, A. et al. Scaling-up biodiversity-ecosystem functioning research. *Ecol. Lett.* **23**, 757–776 (2020).
13. Thompson, P. L. & Gonzalez, A. Ecosystem multifunctionality in metacommunities. *Ecology* **97**, 2867–2879 (2016).

14. Geijzendorffer, I. R. & Roche, P. K. The relevant scales of ecosystem services demand. *Ecosyst. Serv.* **10**, 49–51 (2014).
15. Isbell, F. et al. Linking the influence and dependence of people on biodiversity across scales. *Nature* **546**, 65–72 (2017).
16. Herricks, E. E. Watershed management and protection—issues of scale and process in ecosystems. in *Watershed Management*, 17–28 (American Society of Civil Engineers, 2012).
17. Bond, E. M. & Chase, J. M. Biodiversity and ecosystem functioning at local and regional spatial scales. *Ecol. Lett.* **5**, 467–470 (2002).
18. Hooper, D. U. et al. Effects of biodiversity on ecosystem functioning: a consensus of current knowledge. *Ecol. Monogr.* **75**, 3–35 (2005).
19. Oliver, T. H. et al. Biodiversity and resilience of ecosystem functions. *Trends Ecol. Evol.* **30**, 673–684 (2015).
20. Silva, L. C. R. & Lambers, H. Soil-plant-atmosphere interactions: structure, function, and predictive scaling for climate change mitigation. *Plant Soil* **461**, 5–27 (2021).
21. Hwang, T., Band, L. & Hales, T. C. Ecosystem processes at the watershed scale: extending optimality theory from plot to catchment. *Water Resour. Res.* **45**, W11425 (2009).
22. Band, L. E., Patterson, P., Nemani, R. & Running, S. W. Forest ecosystem processes at the watershed scale: incorporating hillslope hydrology. *Agric. For. Meteorol.* **63**, 93–126 (1993).
23. Yu, X. & Duffy, C. J. Watershed hydrology: scientific advances and environmental assessments. *Water* **10**, 288 (2018).
24. Loreau, M., Mouquet, N. & Holt, R. D. Meta-ecosystems: a theoretical framework for a spatial ecosystem ecology. *Ecol. Lett.* **6**, 673–679 (2003).
25. Hammill, E. et al. Landscape heterogeneity strengthens the relationship between β-diversity and ecosystem function. *Ecology* **99**, 2467–2475 (2018).
26. Strayer, D. L. Challenges in understanding the functions of ecological heterogeneity. in (eds Lovett, G. M., Turner, M. G., Jones, C. G. & Weathers, K. C.) *Ecosystem Function in Heterogeneous Landscapes*, 411–425 (Springer, 2005).
27. Black, P. E. Watershed functions. *J. Am. Water Resour. Assoc.* **33**, 1–11 (1997).
28. Bormann, F. H. & Likens, G. E. Nutrient cycling. *Science* **155**, 424–429 (1967).
29. Gudmundsson, L., Do, H. X., Leonard, M. & Westra, S. The global streamflow indices and metadata archive (GSIM)—part 2: quality control, time-series indices and homogeneity assessment. *Earth Syst. Sci. Data* **10**, 787–804 (2018).
30. Do, H. X., Gudmundsson, L., Leonard, M. & Westra, S. The global streamflow indices and metadata archive (GSIM)—part 1: the production of a daily streamflow archive and metadata. *Earth Syst. Sci. Data* **10**, 765–785 (2018).
31. Przepióra, F. & Ciach, M. Tree microhabitats in natural temperate riparian forests: an ultra-rich biological complex in a globally vanishing habitat. *Sci. Total Environ.* **803**, 149881 (2022).
32. Beugnon, R. et al. Microclimate modulation: an overlooked mechanism influencing the impact of plant diversity on ecosystem functioning. *Glob. Change Biol.* **30**, e17214 (2024).
33. Gravuer, K., Eskelinen, A., Winbourne, J. B. & Harrison, S. P. Vulnerability and resistance in the spatial heterogeneity of soil microbial communities under resource additions. *Proc. Natl. Acad. Sci. USA.* **117**, 7263–7270 (2020).
34. Lovett, G. M., Jones, C. G., Turner, M. G. & Weathers, K. C. eds. Ecosystem function in heterogeneous landscapes. in *Ecosystem Function in Heterogeneous Landscapes*,1–4 (Springer, 2005).
35. Peters, D. P. et al. Living in an increasingly connected world: a framework for continental-scale environmental science. *Front. Ecol. Environ.* **6**, 229–237 (2008).
36. Deng, X. et al. Forest biodiversity increases productivity via complementarity from greater canopy structural complexity. *Proc. Natl. Acad. Sci. USA.* **122**, e2506750122 (2025).
37. Ishii, H. T., Tanabe, S. & Hiura, T. Exploring the relationships among canopy structure, stand productivity, and biodiversity of temperate forest ecosystems. *For. Sci.* **50**, 342–355 (2004).
38. Li, W. et al. Regulation of the global carbon and water cycles through vegetation structural and physiological dynamics. *Environ. Res. Lett.* **19**, 073008 (2024).
39. Poulson, T. L. & Platt, W. J. Gap light regimes influence canopy tree diversity. *Ecology* **70**, 553–555 (1989).
40. Zhu, J. et al. Changing patterns of global nitrogen deposition driven by socio-economic development. *Nat. Commun.* **16**, 46 (2025).
41. Augusto, L. & Boča, A. Tree functional traits, forest biomass, and tree species diversity interact with site properties to drive forest soil carbon. *Nat. Commun.* **13**, 1097 (2022).
42. Lozano-Baez, S. E. et al. Land restoration by tree planting in the tropics and subtropics improves soil infiltration, but some critical gaps still hinder conclusive results. *For. Ecol. Manag.* **444**, 89–95 (2019).
43. Schwendenmann, L., Pendall, E., Sanchez-Bragado, R., Kunert, N. & Hölscher, D. Tree water uptake in a tropical plantation varying in tree diversity: interspecific differences, seasonal shifts and complementarity. *Ecohydrology* **8**, 1–12 (2015).
44. Wu, X. et al. The relationship between species richness and biomass changes from boreal to subtropical forests in China. *Ecography* **38**, 602–613 (2015).
45. Xu, S. et al. Species richness promotes ecosystem carbon storage: evidence from biodiversity-ecosystem functioning experiments. *Proc. R. Soc. B Biol. Sci.* **287**, 20202063 (2020).
46. Chen, C., Xiao, W. & Chen, H. Y. H. Meta-analysis reveals global variations in plant diversity effects on productivity. *Nature* **638**, 435–440 (2025).
47. Liang, J., Zhou, M., Tobin, P. C., McGuire, A. D. & Reich, P. B. Biodiversity influences plant productivity through niche–efficiency. *Proc. Natl. Acad. Sci. USA.* **112**, 5738–5743 (2015).
48. Morin, X., Fahse, L., Scherer-Lorenzen, M. & Bugmann, H. Tree species richness promotes productivity in temperate forests through strong complementarity between species. *Ecol. Lett.* **14**, 1211–1219 (2011).
49. Cardinale, B. J. et al. The functional role of producer diversity in ecosystems. *Am. J. Bot.* **98**, 572–592 (2011).
50. Chisholm, R. A. et al. Scale-dependent relationships between tree species richness and ecosystem function in forests. *J. Ecol.* **101**, 1214–1224 (2013).
51. Li, Y. et al. Early positive effects of tree species richness on soil organic carbon accumulation in a large-scale forest biodiversity experiment. *J. Plant Ecol.* **12**, 882–893 (2019).
52. Shmida, A. & Wilson, M. V. Biological determinants of species diversity. *J. Biogeogr.* **12**, 1–20 (1985).
53. Cardinale, B. J. et al. Effects of biodiversity on the functioning of trophic groups and ecosystems. *Nature* **443**, 989–992 (2006).
54. Jačka, L., Walmsley, A., Kovář, M. & Frouz, J. Effects of different tree species on infiltration and preferential flow in soils developing at a clayey spoil heap. *Geoderma* **403**, 115372 (2021).
55. Craine, J. M. & Dybzinski, R. Mechanisms of plant competition for nutrients, water and light. *Funct. Ecol.* **27**, 833–840 (2013).
56. Farooq, M., Wahid, A., Kobayashi, N., Fujita, D. & Basra, S. M. A. Plant drought stress: effects, mechanisms and management. *Agron. Sustain. Dev.* **29**, 185–212 (2009).
57. González de Andrés, E. et al. Tree-to-tree competition in mixed European beech–Scots pine forests has different impacts on growth and water-use efficiency depending on site conditions. *J. Ecol.* **106**, 59–75 (2018).
58. Nambiar, E. K. S. & Sands, R. Competition for water and nutrients in forests. *Can. J. For. Res.* https://doi.org/10.1139/x93-247 (2011).
59. Liang, J. et al. Co-limitation towards lower latitudes shapes global forest diversity gradients. *Nat. Ecol. Evol.* **6**, 1423–1437 (2022).

60. Lehner, B. & Grill, G. Global river hydrography and network routing: Baseline data and new approaches to study the world's large river systems. *Hydrol. Process.* **27**, 2171–2186 (2013).
61. Hansen, M. C. et al. High-resolution global maps of 21st-century forest cover change. *Science,* https://doi.org/10.1126/science.1244693 (2013).
62. Friedl, M. & Sulla-Menashe, D. MODIS/Terra+Aqua land cover type yearly L3 global 500 m SIN grid V061. NASA EOSDIS Land Processes Distributed Active Archive Center, https://doi.org/10.5067/MODIS/MCD12Q1.061 (2022).
63. Running, S., Mu, Q. & Zhao, M. MODIS/Terra gross primary productivity 8-day L4 global 500 m SIN grid V061. NASA EOSDIS Land Processes Distributed Active Archive Center https://doi.org/10.5067/MODIS/MOD17A2H.061 (2021).
64. Spawn, S. A., Sullivan, C. C., Lark, T. J. & Gibbs, H. K. Harmonized global maps of above and belowground biomass carbon density in the year 2010. *Sci. Data* **7**, 112 (2020).
65. Poggio, L. et al. SoilGrids 2.0: producing soil information for the globe with quantified spatial uncertainty. *SOIL* **7**, 217–240 (2021).
66. Abatzoglou, J. T., Dobrowski, S. Z., Parks, S. A. & Hegewisch, K. C. TerraClimate, a high-resolution global dataset of monthly climate and climatic water balance from 1958-2015. *Sci. Data* **5**, 170191 (2018).
67. Running, S., Mu, Q., Zhao, M. & Moreno, A. MODIS/Terra net evapotranspiration gap-filled 8-day L4 global 500 m SIN grid V061. NASA EOSDIS Land Processes Distributed Active Archive Center, https://doi.org/10.5067/MODIS/MOD16A2GF.061 (2021).
68. Chen, Y., Feng, X. & Fu, B. An improved global remote-sensing-based surface soil moisture (RSSSM) dataset covering 2003–2018. *Earth Syst. Sci. Data* **13**, 1–31 (2021).
69. Gupta, S., Borrelli, P., Panagos, P. & Alewell, C. An advanced global soil erodibility (K) assessment including the effects of saturated hydraulic conductivity. *Sci. Total Environ.* **908**, 168249 (2024).
70. Wu, Q. geemap: a Python package for interactive mapping with Google Earth Engine. *J. Open Source Softw.* **5**, 2305 (2020).
71. Hu, W. et al. Aridity-driven shift in biodiversity–soil multifunctionality relationships. *Nat. Commun.* **12**, 5350 (2021).
72. Jiao, S., Lu, Y. & Wei, G. Soil multitrophic network complexity enhances the link between biodiversity and multifunctionality in agricultural systems. *Glob. Change Biol.* **28**, 140–153 (2022).
73. Schuldt, A. et al. Biodiversity across trophic levels drives multifunctionality in highly diverse forests. *Nat. Commun.* **9**, 2989 (2018).
74. van der Plas, F. et al. Jack-of-all-trades effects drive biodiversity–ecosystem multifunctionality relationships in European forests. *Nat. Commun.* **7**, 11109 (2016).
75. Byrnes, J. E. K. et al. Investigating the relationship between biodiversity and ecosystem multifunctionality: challenges and solutions. *Methods Ecol. Evol.* **5**, 111–124 (2014).
76. Manning, P. et al. Redefining ecosystem multifunctionality. *Nat. Ecol. Evol.* **2**, 427–436 (2018).
77. Myneni, R., Knyazikhin, Y. & Park, T. MODIS/Terra leaf area index/FPAR 8-day L4 global 500 m SIN grid V061. NASA EOSDIS Land Processes Distributed Active Archive Center, https://doi.org/10.5067/MODIS/MOD15A2H.061 (2021).
78. DiMiceli, C., Sohlberg, R. & Townshend, J. MODIS/Terra vegetation continuous fields yearly L3 global 250 m SIN grid v061. NASA EOSDIS Land Processes Distributed Active Archive Center, https://doi.org/10.5067/MODIS/MOD44B.061 (2022).
79. Crowther, T. W. et al. Mapping tree density at a global scale. *Nature* **525**, 201–205 (2015).
80. Potapov, P. et al. Mapping global forest canopy height through integration of GEDI and Landsat data. *Remote Sens. Environ.* **253**, 112165 (2021).
81. Yamazaki, D. et al. A high-accuracy map of global terrain elevations. *Geophys. Res. Lett.* **44**, 5844–5853 (2017).
82. Amatulli, G., McInerney, D., Sethi, T., Strobl, P. & Domisch, S. Geomorpho90m, empirical evaluation and accuracy assessment of global high-resolution geomorphometric layers. *Sci. Data* **7**, 162 (2020).
83. García-Palacios, P., Gross, N., Gaitán, J. & Maestre, F. T. Climate mediates the biodiversity–ecosystem stability relationship globally. *Proc. Natl. Acad. Sci. USA.* **115**, 8400–8405 (2018).

Acknowledgements

We gratefully acknowledge the following researchers for providing valuable data for this analysis: Alexander C. Vibrans, Andrzej M. Jagodzinski, Andy Marshall, Bernhard Schmid, Boknam Lee, Bonaventure Sonké, Bruno Hérault, Christelle Gonmadje, Christian S. Eljatib, Christian Ammer, Christopher Baraloto, Damiano Gianelle, Daniel Piotto, David A. Coomes, David E. Odeke, David Verbyla, Emanuel H. Martin, Eric B. Searle, Ernst-Detlef Schulze, Eungul Lee, Fernando Valladares, Filippo Bussotti, Francesco Rovero, Frédéric Mortier, Fumiaki Kitahara, Geerten M. Hengeveld, Hans Pretzsch, Helge Bruelheide, Huicui Lu, Hyun-Seok Kim, Jacek Oleksyn, Jordi Vayreda, Leandro V. Ferreira, Leena Finér, Lorenzo Frizzera, Markus Fischer, Mart-Jan Schelhaas, Michael R. Ngugi, Miina Rautiainen, Mo Zhou, Nestor E. Obiang, Nurdin Chamuya, Olivier Bouriaud, Pascal A. Niklaus, Patricia Alvarez-Loayza, Peri P. Luis, Radomir Bałazy, Rebecca Tavani, Renato Valencia, Robert Bitariho, Rodolfo M. Vasquez, Susan Wiser, Susanne Brandl, Sylvie Gourlet-Fleury, Terry Sunderland, Timothy O'Brien, Tomasz Zawiła-Niedźwiecki, Tommaso Jucker, Verginia Wortel, Victor J. Neldner, and William Marthy, Xiangdong Lei, and other members of the Global Forest Biodiversity Initiative for their generous data contribution, which is essential to the completion of this study. The international collaboration underpinning this study was supported by the Science-i cyberinfrastructure (https://science-i.org/). This research was supported by the National Natural Science Foundation of China (Nos. 32401373, 32430068, and 32471650), Youth Innovation Promotion Association CAS (No. Y2022091), and the Chinese Academy of Sciences.

Author contributions

K.Z. designed the research, conducted the analysis, and wrote the manuscript. J.Z., C.S., Y.Z., X.W., T.H., and Q.Z. collected samples, conducted analysis, and wrote the manuscript. J.L., P.B.R., G.-J.N., H.Y.H.C., J.D., M.S.-L., A.P., H.V., G.A., E.P., N.T., T.W.C., S.d.-M., S.P., P.S., B.J., P.L.P., and N.P. provided data for the analysis. All authors assisted in the discussion of the results and preparation of the manuscript.

Competing interests

The authors declare no competing interests.

Additional information

Supplementary information The online version contains Supplementary material available at https://doi.org/10.1038/s41467-026-74914-z.

Correspondence and requests for materials should be addressed to Quanfa Zhang or Kerong Zhang.

Peer review information *Nature Communications* thanks the anonymous reviewers for their contribution to the peer review of this work. A peer review file is available.

[1]State Key Laboratory of Lake and Watershed Science for Water Security, Wuhan Botanical Garden, Chinese Academy of Sciences, Wuhan, PR China. [2]Department of Forest Resources, University of Minnesota, St. Paul, MN, USA. [3]Hawkesbury Institute for the Environment, Western Sydney University, Penrith, NSW, Australia. [4]Institute for Global Change Biology and School for Environment and Sustainability, University of Michigan, Ann Arbor, MI, USA. [5]Department of Geography, University of North Carolina at Chapel Hill, Chapel Hill, NC, USA. [6]Division of Earth and Climate Sciences, Nicholas School of the Environment, Duke University, Durham, NC, USA. [7]Eastern Forest Environmental Threat Assessment Center, Southern Research Station, USDA Forest Service, Research Triangle Park, NC, USA. [8]Faculty of Natural Resources Management, Lakehead University, Thunder Bay, ON, Canada. [9]Wageningen University and Research, Wageningen, The Netherlands. [10]Hubei Key Laboratory of Wetland Evolution & Ecological Restoration, Wuhan Botanical Garden, Chinese Academy of Sciences, Wuhan, China. [11]Danjiangkou Wetland Ecosystem Field Scientific Observation and Research Station, The Chinese Academy of Sciences & Hubei Province, Wuhan, China. [12]Institute of Botany, The Czech Academy of Sciences, Třeboň, Czechia. [13]Geobotany, Faculty of Biology, University of Freiburg, Freiburg im Breisgau, Germany. [14]Centre for Forest Research, Université du Québec à Montréal, Montréal, QC, Canada. [15]CERNAS-IPV Research Centre, Campus Politécnico, Repeses, Polytechnic Institute of Viseu, Viseu, Portugal. [16]Centre for the Research and Technology of Agro-Environmental and Biological Sciences, CITAB, University of Trás-os-Montes and Alto Douro, UTAD, Vila Real, Portugal. [17]Department of Agricultural, Food, Environmental and Animal Sciences, University of Udine, Udine, Italy. [18]V. N. Sukachev Institute of Forest, FRC KSC, Siberian Branch of the Russian Academy of Sciences, Krasnoyarsk, Russia. [19]Department of Forestry and Natural Resources, Purdue University, West Lafayette, IN, USA. [20]Institute of Integrative Biology, ETH Zurich (Swiss Federal Institute of Technology), Zurich, Switzerland. [21]Department of Agricultural and Forest Sciences and Engineering, University of Lleida, Lleida, Spain. [22]Forest Science and Technology Centre of Catalonia (CTFC), Solsona, Spain. [23]School of Social Sciences (Urban Studies), Western Sydney University, Penrith, NSW, Australia. [24]Silviculture and Forest Ecology of the Temperate Zones, University of Göttingen, Göttingen, Germany. [25]Białowieża Geobotanical Station, Faculty of Biology, University of Warsaw, Białowieża, Poland. [26]Universidad Nacional de la Patagonia Austral (UNPA), Instituto Nacional de Tecnología Agropecuaria (INTA), Consejo Nacional de Investigaciones Científicas y Técnicas (CONICET), Río Gallegos, Argentina. [27]GIP Ecofor, Paris, France. [28]School of Ecology and Environment, Tibet University, Lhasa, China. ✉e-mail: qzhang@wbgcas.cn; kerongzhang@wbgcas.cn